CHEMISTRY
A EUROPEAN JOURNAL

DOI: 10.1002/chem.200800383

Bis(amido)cyclodiphosph(III)azane Complexes of Yttrium and the Lanthanides

Marcus Rastätter,[a] Roberto B. Muterle,[a] Peter W. Roesky,*[a, b] and Sven K.-H. Thiele[c]

Abstract: The first cyclodiphosph(III)azane complexes of the rare-earth elements have been synthesized. Reactions of the lithium salt *cis*-[(*t*BuNP)$_2$(*t*BuN)$_2${Li(thf)}$_2$] with anhydrous yttrium trichloride or the heavier lanthanide trichlorides resulted in the corresponding cyclodiphosph(III)azane complexes [Li(thf)$_4$][{(*t*BuNP)$_2$-(*t*BuN)$_2$}LnCl$_2$] (Ln = Y (**1a**), Ho (**1b**), Er (**1c**)). The single-crystal X-ray structures showed that compounds **1a–c** consisted of ion pairs composed of a [Li(thf)$_4$]$^+$ cation and a C_{2v} symmetric [{(*t*BuNP)$_2$(*t*BuN)$_2$}LnCl$_2$]$^-$ anion. By treating *cis*-[(*t*BuNP)$_2$(*t*BuN)$_2${Li(thf)}$_2$] with anhydrous SmCl$_3$ in THF, the trimetallic complex [{(*t*BuNP)$_2$(*t*BuN)$_2$}-SmCl$_3$Li$_2$(thf)$_4$] (**2**) was obtained. The influence of the ionic radii of the lanthanides can be seen in the single-crystal X-ray structure of compound **2**, which forms a six-membered Cl-Li-Cl-Li-Cl-Sm metallacycle. The ring adopts a boat conformation in which one chlorine atom and the samarium atom are displaced from the Cl$_2$Li$_2$ least-square plane. Heating of the metalate complexes in toluene resulted in the extrusion of lithium chloride and the formation of the neutral dimeric metal chloride complexes of the composition [(*t*BuNP)$_2$(*t*BuN)$_2$LnCl(thf)]$_2$ (Ln = Y (**3a**), La (**3b**) Nd (**3c**), Sm (**3d**)). Furthermore, treating **1a** with KNPh$_2$ resulted in a lithium metalate complex of the composition [Li(thf)$_4$][{(*t*BuNP)$_2$-(*t*BuN)$_2$}Y(NPh$_2$)$_2$] (**4**). The coordination mode of the {(*t*BuNP)$_2$(*t*BuN)$_2$}$^{2-}$ ligand in **4** is different to that observed in **1a–c**, **2**, and **3a–d**; instead of a symmetric η^2 coordination of the ligand, a heterocubane-type structure is observed in the solid state. The complex [(*t*BuNP)$_2$(*t*BuN)$_2$NdCl(thf)] (**3c**) was used as a Ziegler–Natta catalyst for the polymerization of 1,3-butadiene to poly-*cis*-1,4-butadiene. The observed activities of the Ziegler–Natta catalyst strongly depended upon the nature of the cocatalyst; in some case very high turnover rates and a *cis* selectivity of 93–94 % were observed.

Keywords: cage compounds · chelates · lanthanides · N,P ligands · polymerization

Introduction

Recently there has been significant interest in the area of d- and f-transition-metal chemistry to substitute the well-established cyclopentadienyl ligand[1] by anionic nitrogen-based ligand systems.[2] In lanthanide chemistry one possible approach is the use of inorganic amides. Since phosphorus and nitrogen form compounds of greater structural diversity than any other congeners in the periodic table, N,P systems, such as phosphinimides (R$_2$PNR′),[3] phosphoraneiminates (R$_3$PN),[4] diphosphanylamide, {(Ph$_2$P)$_2$N}$^-$,[5,6] phosphiniminomethanides ((RNPR′$_2$)CH),[7] phosphiniminomethandiides ((RNPR′$_2$)C),[8] and diiminophosphinates (R$_2$P(NR′)),[9] have been widely used as ligands for the lanthanides. These investigations have shown that lanthanide complexes with N,P ligands may not only exhibit unusual coordination modes, but they may also be catalytically active for the polymerization of ε-caprolactone[5,10] and methyl methacrylate,[11] hydroamination cyclization,[12] hydrosilylation, and the sequential hydroamination/hydrosilylation reaction.[13] For this reason we were attracted to the bis(amido)cyclodiphosph(III)azanes (Scheme 1), which are known to act as dinegative chelating N-donor ligands. Cyclodiphosph(III)azanes have been known for more than a century,[14] but were only fully characterized in the

[a] Dr. M. Rastätter, R. B. Muterle, Prof. Dr. P. W. Roesky
Institut für Chemie und Biochemie
Freie Universität Berlin
Fabeckstrasse 34-36, 14195 Berlin (Germany)
[b] Prof. Dr. P. W. Roesky
Institut für Anorganische Chemie
Universität Karlsruhe (TH)
Engesserstr. 15, 76128 Karlsruhe (Germany)
Fax: (+49) 721-608-4845
E-mail: roesky@chemie.uni-karlsruhe.de
[c] Dr. S. K.-H. Thiele
Dow Olefinverbund GmbH, Synthetic Rubber Business
PF1163, 06201, Merseburg (Germany)

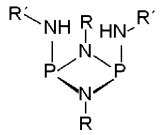

Scheme 1.

1970s.[15,16] Their preparation is usually based on the reaction of PCl_3 with an excess of a free amine.[17,18] Today cyclodiphosph(III)azanes are well established as anionic N-donor ligands in main-group[18,19,20] and early-transition-metal chemistry.[21,22] Group 4 complexes of these ligands have been shown to have high activities in ethylene polymerization in the presence of methylaluminoxane (MAO). Thus, cyclodiphosph(III)azanes can be considered as alternatives to bridged biscyclopentadienyl ligands in *ansa*-metallocenes. An advantage of using cyclodiphosph(III)azanes ligands in post-metallocene chemistry is the easy modulation of their steric demand by the use of different amines.

In contrast to the well-established main-group and early-transition-metal chemistry of cyclodiphosph(III)azanes, complexes of the f elements are not mentioned in the literature. Herein we report the synthesis, structural characterization, and the application in the polymerization of 1,3-butadiene of the first cyclodiphosph(III)azane complexes of yttrium and the lanthanides. As a result of the larger ionic radii of the rare-earth elements, significant differences in the coordination polyhedra compared to main-group and early-transition-metal complexes are observed in some cases.

Results and Discussion

Metalate complexes: As a transfer reagent for the dianionic *cis*-bis(amino)cyclodiphosph(III)azane ligand, the corresponding lithium salt *cis*-$[(t\text{BuNP})_2(t\text{BuN})_2\{\text{Li(thf)}\}_2]$, which was reported earlier in the literature,[18] was used. Transmetallation of *cis*-$[(t\text{BuNP})_2(t\text{BuN})_2\{\text{Li(thf)}\}_2]$ with anhydrous yttrium or the heavier lanthanide trichlorides in a 1:1 molar ratio in THF, followed by extraction with toluene resulted in the corresponding cyclodiphosph(III)azane complexes $[\text{Li(thf)}_4][\{(t\text{BuNP})_2(t\text{BuN})_2\}\text{LnCl}_2]$ (Ln = Y (**1a**), Ho (**1b**), Er (**1c**); Scheme 2). The new complexes have been characterized by standard analytical/spectroscopic techniques and the solid-state structures of all three compounds were established by single-crystal X-ray diffraction (Figure 1).

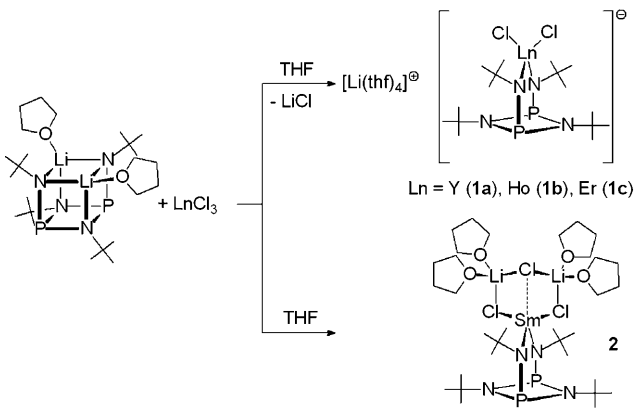

Scheme 2.

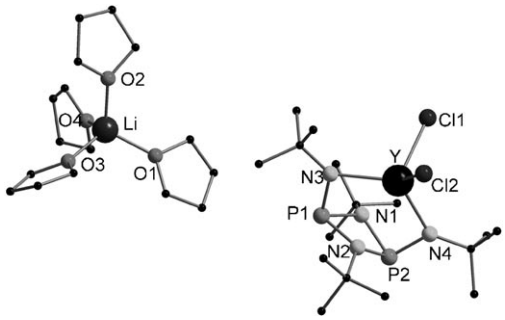

Figure 1. Solid-state structure of **1a** showing the atom labeling scheme, omitting hydrogen atoms. Selected bond lengths [pm] or angles [°] (also given for the isostructural **1b** and **1c**): **1a**: Y–N3 = 228.7(5), Y–N4 = 226.4(5), Y–Cl1 = 256.3(2), Y–Cl2 = 256.3(2), P1–N1 = 177.9(4), P1–N2 = 178.4(5), P1–N3 = 164.3(5), P2–N1 = 177.8(5), P2–N2 = 178.55), P2–N4 = 164.4(5), P1–P2 = 272.9(0); Cl1-Y-Cl2 = 100.79(7), N3-Y-N4 = 123.0(2), Y-N3-P1 = 95.2(2), Y-N4-P2 = 96.2(2), N1-P1-N2 = 77.7(2), N1-P2-N2 = 77.7(2). **1b**: Ho–N3 = 227.5(3), Ho–N4 = 226.3(3), Ho–Cl1 = 255.71(9), Ho–Cl2 = 255.92(10), P1–N1 = 177.8(3), P1–N2 = 177.9(3), P1–N3 = 164.7(3), P2–N1 = 178.2(3), P2–N2 = 177.6(3), P2–N4 = 164.4(3), P1–P2 = 272.9(5); Cl1-Ho-Cl2 = 101.27(4), N3-Ho-N4 = 123.16(10), Ho-N3-P1 = 95.62(12), Ho-N4-P2 = 96.11(13), N1-P1-N2 = 77.60(12), N1-P2-N2 = 77.56(11). **1c**: Er–N3 = 226.7(3), Er–N4 = 225.2(3), Er–Cl1 254.32(11), Er–Cl2 254.50(10), P1–N1 178.1(3), P1–N2 = 177.5(3), P1–N3 = 164.5(3), P2–N4 = 164.5(3), P2–N1 = 178.0(3), P2–N2 = 178.1(3), P1–P2 = 272.7(3); Cl1-Er-Cl2 = 101.25(4), N3-Er-N4 = 123.71(10), Er-N3-P1 = 95.38(13), Er-N4-P2 = 95.97(13), N1-P1-N2 = 77.74(13), N1-P2-N2 = 77.62(12).

Crystals of compounds **1a–c**, which consist of ion pairs composed of a $[\text{Li(thf)}_4]^+$ cation and a $[\{(t\text{BuNP})_2(t\text{BuN})_2\}\text{LnCl}_2]^-$ anion, are isomorphous. They crystallize in the orthorhombic space group *Pbca* and have eight molecules in the unit cell. The formation of metalate complexes in lanthanide chemistry is quite common.[23,24,25] The C_{2v} symmetric $[\{(t\text{BuNP})_2(t\text{BuN})_2\}\text{LnCl}_2]^-$ anion has a noncrystallographic C_2 axis through the lanthanide atom and the center of the P_2N_2 plane and a noncrystallographic mirror plane through N1, N2, Cl1, and Cl2. The anion is isoelectronic to the corresponding Group 4 complexes $[\{(t\text{BuNP})_2(t\text{BuN})_2\}\text{MCl}_2]$ (M = Ti, Zr, Hf).[21,22] Within the $[\{(t\text{BuNP})_2(t\text{BuN})_2\}\text{LnCl}_2]^-$ anion the Ln–N bond lengths are in the expected range: Y–N3 228.7(5) and Y–N4 226.4(5) pm in **1a**, Ho–N3 = 227.5(3) and Ho–N4 = 226.3(3) in **1b**, and Er–N3 226.7(3) and Er–N4 = 225.2(3) pm in **1c**. The bite angles N3-Ln-N4 of the ligand are 123.0(2) in **1a**, 123.16(10) in **1b**, and 123.71(10)° in **1c**. In comparison with the neutral cyclodiphosph(III)azane $\{(t\text{BuNP})_2(t\text{BuNH})_2\}$ the $\{(t\text{BuNP})_2(t\text{BuN})_2\}^{2-}$ moiety in compounds **1a–c** is elongated along the P–P axis (P1–P2 = 272.9(0) pm (**1a**), P1–P2 = 272.9(5) (**1b**), P1–P2 = 272.7(3) pm (**1c**) versus 260.0(2) pm in $\{(t\text{BuNP})_2(t\text{BuNH})_2\}$).[18] The Li metal center of the cations in compounds **1a–c** are tetrahedrally coordinated by four THF molecules; a common structural motif.[25]

The NMR spectra of the diamagnetic compound **1a** were investigated and are in agreement with the solid-state structures. The ^{1}H NMR spectrum of compound **1a** shows two characteristic sharp singlets of the *tert*-butyl groups at $\delta =$ 1.26 and 1.39 ppm. In the ^{31}P{^{1}H} NMR spectrum one typical signal for the $\{(t\text{BuNP})_2(t\text{BuN})_2\}^{2-}$ ligand is observed at $\delta =$ 91.6 ppm, which is in the range of comparable Group 4 complexes, such as $[\{(t\text{BuNP})_2(t\text{BuN})_2\}\text{HfCl}_2]$ ($\delta =$ 102.03 ppm).[22]

Besides the heavier lanthanides, we also studied the reaction of the *cis*-bis(amino)cyclodiphosph(III)azane ligand with samarium, which is lighter and larger. By treating *cis*-$[(t\text{BuNP})_2(t\text{BuN})_2\{\text{Li(thf)}\}_2]$ with anhydrous $SmCl_3$ in THF, followed by extraction with toluene, the trimetallic complex $[\{(t\text{BuNP})_2(t\text{BuN})_2\}\text{SmCl}_3\text{Li}_2(\text{thf})_4]$ (**2**) was isolated (Scheme 2). The influence of the ionic radii of the lanthanides can be seen in the single-crystal X-ray structure of compound **2**, which crystallizes in the monoclinic space group $P2_1/c$ with four molecules in the unit cell (Figure 2). Compound **2** consists of a $[\{(t\text{BuNP})_2(t\text{BuN})_2\}\text{SmCl}]$ subunit to which two equivalents of LiCl are coordinated. In contrast to **1a–c**, which have separate ion pairs, the lithium atoms of compound **2**, which form a distorted tetrahedral coordination polyhedron, are surrounded by two chlorine atoms and two THF molecules. Thus, a six-membered Cl-Li-Cl-Li-Cl-Sm metallacycle is formed. The ring adopts a boat conformation, in which the chlorine atom Cl3 and the samarium atom are displaced from the Cl_2Li_2 least-squares plane. Therefore, the chlorine atom Cl3 shows only a weak interaction with the samarium atom. The Sm–Cl3 distance of 291.8(2) pm is significantly longer than the Sm–Cl1 (274.2(2) pm) and the Sm–Cl2 (274.3(2) pm) distances. A similar conformation had previously been observed in the allenyl/propargyl-complex $[\{\{(\text{Me}_3\text{Si})_2(\text{C}_5\text{H}_2)\}\text{SiMe}_2(\eta^3\text{-C=C=C[H]SiMe}_3)\}\text{SmCl}_3\text{Li}_2(\text{tmeda})_2]$ (TMEDA = tetramethylethylenediamine).[26] As observed in compounds **1a–c**, the $\{(t\text{BuNP})_2(t\text{BuN})_2\}^{2-}$ ligand in **2** coordinates in an η^2 fashion through the two anionic nitrogen atoms onto the samarium metal (Sm–N3 = 233.2(5) and Sm–N4 = 234.2(6) pm). Again the $\{(t\text{BuNP})_2(t\text{BuN})_2\}^{2-}$ moiety of **2** is elongated along the P1–P2 axis (P1 < C-P2 = 271.56(2) pm) relative to that of $\{(t\text{BuNP})_2(t\text{BuNH})_2\}$ (260.0(2) pm).[18]

Neutral chloride complexes: To avoid the formation of "ate" complexes we were interested in finding another synthetic protocol. One way to achieve this is by the use of potassium instead of lithium reagents. Although the incorporation of potassium chloride is sometimes observed in lanthanide chemistry,[6a,24,27] it is far less common than the formation of "ate" complexes seen when using lithium reagents.[23] Unfortunately, attempts to deprotonate *cis*-$[(t\text{BuNP})_2(t\text{BuNH})_2]$ with the alkali-metal benzyls ($PhCH_2M$ (M = Na, K)) to form the corresponding $\{(t\text{BuNP})_2(t\text{BuN})_2\}\text{M}_2$ complexes failed and only the monomeric anion $[(t\text{BuN})_2\text{P}]^-$ was obtained.[28] Since no suitable potassium reagent was available, we again treated the lithium compound *cis*-$[(t\text{BuNP})_2(t\text{BuN})_2\{\text{Li(thf)}\}_2]$ with the lanthanide trichlorides in a 1:1 molar ratio in THF, but after extraction with toluene the resulting mixture was heated at reflux for some time. Upon heating, the precipitation of lithium chloride was observed and the neutral dimeric complexes $[(t\text{BuNP})_2(t\text{BuN})_2\text{LnCl(thf)}]_2$ (Ln = Y (**3a**), La (**3b**), Nd (**3c**), Sm (**3d**)) were formed (Scheme 3). The rate of decomposition

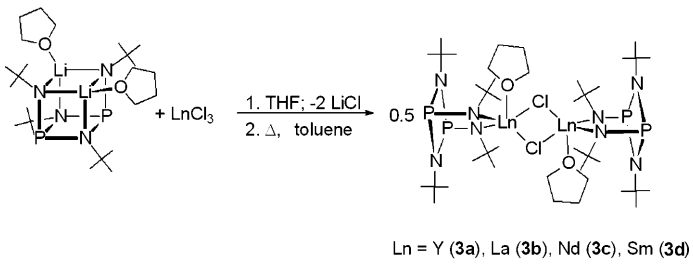

Scheme 3.

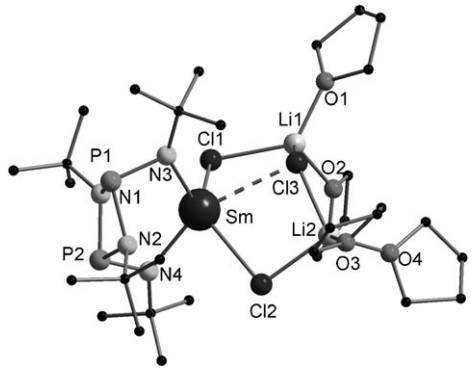

Figure 2. Solid-state structure of **2** showing the atom labeling scheme, omitting hydrogen atoms. Selected bond lengths [pm] or angles [°]: Sm–Cl1 = 274.2(2), Sm–Cl2 = 274.3(2), Sm–Cl3 = 291.8(2), Sm–N3 = 233.2(5), Sm–N4 = 234.2(6), Cl1–Li1 = 231(2), Cl3–Li1 = 235(1), Cl2–Li2 = 227(1), Cl3–Li2 = 234(1), N3–P1 = 165.3(6), N4–P2 = 162.5(7); Cl1-Sm-Cl2 = 123.53(7), N3-Sm-N4 = 119.3(2), Sm-N3-P1 = 96.2(2), Sm-N4-P2 = 96.7(3), Sm-Cl1-Li1 = 94.3(3), Sm-Cl2-Li2 = 96.5(3), Li1-Cl3-Li2 = 125.8(5), Cl1-Li1-Cl3 = 97.2(5), Cl2-Li2-Cl3 = 96.9(5).

of the "ate" complexes depended on the structure of the compounds and thus on the ionic radius. Whereas the neutral yttrium complex must be heated for a long period of time, the corresponding lanthanum, neodymium, and samarium complexes are obtained much faster. The decomposition could be monitored by ^{31}P{^{1}H} NMR spectroscopy. The ^{31}P{^{1}H} NMR signal of **1a** is observed at $\delta = 91.6$ ppm, whereas the signal shifts downfield to $\delta = 99.7$ ppm in **3a**. Complexes **3a–d** were characterized by Raman spectroscopy and elemental analysis, and the ^{1}H and ^{31}P{^{1}H} NMR spectra of the diamagnetic compounds **3a,b** were determined. The ^{1}H NMR spectra of compounds **3a,b** show the two characteristic sharp singlets of the *tert*-butyl groups at $\delta = 1.23$ and 1.37 ppm for **3a** and $\delta = 1.24$ and 1.25 ppm for **3b**. These signals are in similar positions to those of the *tert*-butyl groups in compound **1a**. In the ^{31}P{^{1}H} NMR spectra of compounds **3a,b**, characteristic singlets are observed for the $\{(t\text{BuNP})_2(t\text{BuN})_2\}^{2-}$ ligand at $\delta = 99.7$ (**3a**) and 93.2 ppm (**3b**).

The solid-state structures of **3a–d** were established by single-crystal X-ray diffraction (Figure 3). Compounds **3a–d** crystallize in the triclinic space group $P\bar{1}$ and have one molecule in the unit cell. Whereas the metalate complexes **1a–c** and **2** exhibit two different types of structures, depending on the radius of the metal ion, only one type of structure is detected for the neutral metal complexes **3a–d**.

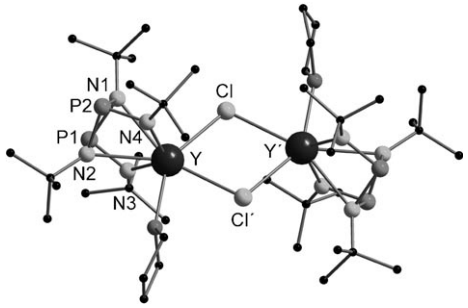

Figure 3. Solid-state structure of **3a** showing the atom labeling scheme, omitting hydrogen atoms. Selected bond lengths [pm] or angles [°] (also given for the isostructural **3b**, **3c**, and **3d**): **3a**: Y1–N3 = 227.2(3), Y–N4 = 225.9(3), Y–Cl = 273.46(10), Y–Cl′ = 273.62(9), Y–O = 242.6(2), P1–N1 = 178.2(3), P1–N2 = 178.0(3), P2–N1 = 178.0(3), P2–N2 = 178.0(3), P1–N3 = 166.0(3), P2–N4 = 166.1(3); Cl-Y-Cl′ = 72.41(3), Cl-Y-O = 144.58(6), Y-N3-P1 = 95.29(12), Y-N4-P2 = 95.79(12), N3-Y-N4 = 123.66(9), Y-Cl-Y′ = 107.59(3), N1-P1-N2 = 78.52(12), N1-P2-N2 = 78.58(12). **3b**: La–N3 = 237.4(6), La–N4 = 236.1(6), La–Cl = 288.1(3), La–Cl′ = 290.1(2), La–O = 261.0(5), P1–N1 = 178.3(6), P1–N2 = 177.8(6), P2–N1 = 177.5(6), P2–N2 = 178.2(6), P1–N3 = 166.6(6), P2–N4 = 166.0(5); Cl-La-Cl = 74.49(8), Cl-La-O = 145.97(12), La-N3-P1 = 97.9(3), La-N4-P2 = 98.7(3), N3-La-N4 = 116.6(2), La-Cl-La = 105.51(8), N1-P1-N2 = 78.7(3), N1-P2-N2 = 78.8(3). **3c**: Nd–N3 = 232.8(4), Nd–N4 = 231.3(3), Nd–O = 256.0(3), Nd–Cl = 281.89(14), Nd–Cl′ = 282.80(13), P1–N1 = 177.9(4), P1–N2 = 177.2(4), P2–N1 = 177.6(3), P2–N2 = 177.8(4), P1–N3 = 166.1(4), P2–N4 = 166.0(4); Cl-Nd-Cl′ = 74.79(5), Cl-Nd-O = 146.48(8), Nd-N3-P1 = 96.0(2), Nd-N4-P2 = 97.6(2), N3-Nd-N4 = 119.52(12), Nd-Cl-Nd′ = 105.21(5), N1-P1-N2 = 78.7(2), N1-P2-N2 = 78.6(2). **3d**: Sm–N3 = 231.1(3), Sm–N4 = 229.6(3), Sm–Cl = 278.69(10), Sm–Cl′ = 280.28(9), Sm–O = 251.3(3), P1–N3 = 166.1(3), P1–N1 = 178.0(3), P1–N2 = 177.6(3), P2–N1 = 177.6(3), P2–N2 = 177.7(3), P2–N4 = 166.6(3); Cl-Sm-Cl′ = 73.80(3), Cl-Sm-O = 145.61(12), Sm-N3-P1 = 96.36(12), Sm-N4-P2 = 96.89(12), N3-Sm-N4 = 120.91(9), Sm-Cl-Sm = 106.20(3), N1-P1-N2 = 78.59(12), N1-P2-N2 = 78.65(12).

The X-ray structures of **3a–d** revealed dimeric complexes in which the metal centers are bridged asymmetrically by two chlorine atoms. A crystallographic inversion center, in the middle of the Ln-Cl-Ln′-Cl′ plane, was observed. A comparison of the Ln-Cl-Ln′ (107.59(3) (**3a**), 105.51(8) (**3b**), 105.21(5) (**3c**), 106.20(3)° (**3d**)) and Cl-Ln-Cl′ angles (72.41(3) (**3a**), 74.49(8) (**3b**), 74.79(5) (**3c**), 73.80(3)° (**3d**)) of the central Ln-Cl-Ln′-Cl′ four-membered rings in compounds **3a–d** show the expected influence of the radius of the metal atom. The metal atoms in compounds **3a–d** are five coordinate, bonding to two nitrogen atoms of the $\{(t\text{BuNP})_2(t\text{BuN})_2\}^{2-}$ ligand, one THF molecule, and two μ-chlorine atoms. Within the series **3a–d**, the bite angle of the $\{(t\text{BuNP})_2(t\text{BuN})_2\}^{2-}$ ligand decreases with an increasing ionic radius (N3-Ln-N4: 123.66(9) (**3a**), 116.6(6) (**3b**), 119.52(12) (**3c**), 120.91(9)° (**3d**)), whereas the Cl-Ln-O angle remains almost constant (144.58(6) (**3a**), 145.97(12) (**3b**), 146.48(8) (**3c**), 145.61(12)° (**3d**)). As observed for the metalate complexes **1a–c**, there is an elongation along the P1–P2 axis relative to *cis*-$[(t\text{BuNP})_2(t\text{BuNH})_2]$.

Amido complex: To learn more about the reactivity of our complexes we were interested in synthesizing an amido derivative. Treating $KNPh_2$ with **1a** in a 1:1 or 2:1 molar ratio in toluene at room temperature did not afford the expected neutral complex of the composition $[\{(t\text{BuNP})_2(t\text{BuN})_2\}\text{YNPh}_2]$, but instead the metalate complex $[\text{Li}(\text{thf})_4][\{(t\text{BuNP})_2(t\text{BuN})_2\}\text{Y}(\text{NPh}_2)_2]$ (**4**) (Scheme 4). Com-

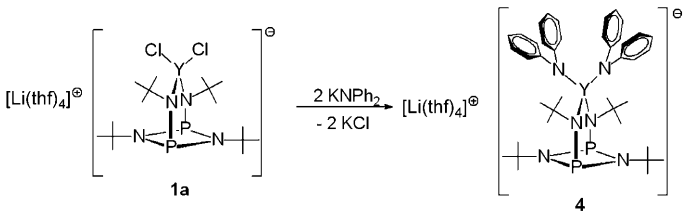

Scheme 4.

pound **4** was characterized by ^{1}H and ^{31}P{^{1}H} NMR spectroscopy, Raman spectroscopy, and elemental analysis. In the ^{1}H NMR spectrum of **4** the phenyl region is not very characteristic, but the two singlets of the *tert*-butyl groups are observed at $\delta = 1.00$ and 1.22 ppm. In the ^{31}P{^{1}H} NMR spectrum of **4** one signal is seen at $\delta = 127.6$ ppm, which is significantly downfield to that of the starting material **1a** ($\delta = 91.6$ ppm).

Compound **4** crystallizes in the monoclinic space group $P2_1/c$ and has four molecules in the unit cell (Figure 4). As was seen for **1a–c**, an ionic structure is formed consisting of a $[\text{Li}(\text{thf})_4]^+$ cation and a $[\{(t\text{BuNP})_2(t\text{BuN})_2\}\text{Y}(\text{NPh}_2)_2]^-$

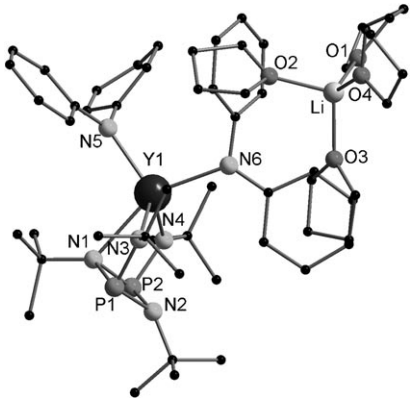

Figure 4. Solid-state structure of **4** showing the atom labeling scheme, omitting hydrogen atoms. Selected bond lengths [pm] or angles [°]: Y–N1 = 254.4(4), Y1–N2 = 337.2(1), Y–N3 = 227.1(5), Y–N4 = 225.3(4), Y–N5 = 229.4(5), Y–N6 = 234.8(5), P1–N1 = 177.0(5), P1–N2 = 172.9(6), P1–N3 = 167.2(5), P2–N1 = 178.0(5), P2–N2 = 173.9(6), P2–N4 = 167.4(5), P1–P2 = 267.1(2); N3-Y-N4 = 108.8(2), N5-Y-N6 = 106.3(2), Y-N3-P1 = 103.5(2), Y-N4-P2 = 103.7(2), P1-N1-P2 = 97.6(2), P1-N2-P2 = 100.7(3), N1-P1-N2 = 81.0(2), N1-P2-N2 = 80.4(2).

anion; the Li metal centre of the cation is tetrahedrally coordinated by four THF molecules. A comparable arrangement was observed in $[Li(thf)_4][(Ph_2N)_4Y]$.[29] In contrast to all other structures described herein, the yttrium atom in **4** is not located above the center of the N_2P_2 plane, but is shifted in the direction of N1. The structure of the anion thus adopts a C_s symmetric heterocubane arrangement. Similar structures of cyclodiphosph(III)azane complexes in main-group chemistry have previously been observed.[18,19] The coordination polyhedron of the pentacoordinated yttrium atom is best described as a distorted trigonal bipyramid with the NPh_2 substituents in the apex and in the plane. As expected the bond length between the neutral nitrogen atom and the yttrium ion (Y−N1 = 254.4(4) pm) is longer than the bond lengths of the corresponding anionic nitrogen atoms (Y−N3 = 227.1(5), Y−N4 = 225.3(4), Y−N5 = 229.4(5), Y−N6 234.8(5) pm)). As a result of the different coordination mode of the yttrium atom, the structure of the $\{(t\text{BuNP})_2(t\text{BuN})_2\}^{2-}$ ligand is altered. Thus, in contrast to the above structures, a compression of the N2P2 ring along the P1–P2 axis in compound **4** is observed (P1−P2 = 267.1(2) vs. 272.9(0) pm for **1a**).

1,3-Butadiene polymerization: Neodymium-containing Ziegler–Natta catalysts for the polymerization of 1,3-butadiene essentially to poly-*cis*-1,4-butadiene have been used in industrial production for some time now.[30,31] In this context (η^3-allyl) neodymium complexes, such as $(\eta^3\text{-}C_3H_5)_3$Nd-(dioxane), $[(\eta^3\text{-}C_3H_5)_2Nd(\mu\text{-Cl})(thf)]_2$, and $(\eta^3\text{-}C_3H_5)NdCl_2$-$(thf)_2$ have been shown to be extremely active and highly selective complex catalysts.[32] To obtain information about the catalytic activity of the novel neodymium complex **3c**, the polymerization of 1,3-butadiene was investigated using this complex as the catalyst in the presence of various cocatalysts with cyclohexane as the solvent at 65 °C. We focused on compound **3c** because only neodymium-based Ziegler–Natta systems play a major role in the industrial polymerization of 1,3-butadiene to poly-*cis*-1,4-butadiene.[30] The results of the polymerization experiments are listed in Table 1. Several cocatalysts and cocatalyst mixtures were used in combination with compound **3c**. The molar ratio of compound **3c** to 1,3-butadiene was in the range of about 19750 to 22100. It can clearly be seen from Table 1 that the observed activity strongly depends on the nature of the cocatalyst. The microstructure was only established for those runs that showed a high activity. In one run using modified methylalumoxane, comprised of trimethylaluminum and triisobutylaluminum (MMAO-3A; 7 wt % solution in heptane (Akzo Nobel)) as the cocatalyst and 1,3-butadiene as the substrate, the catalyst to cocatalyst to substrate ratio of about 1:290:20800 resulted in a *cis* selectivity of 94 %. A turnover frequency of approximately 17000 (mol of Nd)$^{-1}$ h^{-1} was observed (Table 1, run 1). The observed activity is significantly higher than for other published amido neodymium catalysts, such as lithium (hexa-1,5-diene-1,6-diamide)neodymium dibromide,[33] Nd(versatate)$_3$/MAO (1:264),[34] and {[2,6-{[2,6-(*i*Pr)$_2$C$_6$H$_3$]N-C=(CH_2)}$_2$(C_5H_3N)]Nd}(μ-Cl)(μ-X)[Li (thf)$_2$] (X = Cl 53 %, Me 47 %),[35] which were tested under comparable conditions. For example, the third system above shows an activity of 0.74 kg of polymer per (mmol catalyst·h), whereas compound **3c** shows an activity of 0.981 kg of polymer per (mmol catalyst·h) under similar conditions. For the lithium (hexa-1,5-diene-1,6-diamide)neodymium dibromide catalyst an activity of 0.116 kg polymer per (mmol catalyst·h) was reported under comparable conditions. In all cases the *cis* selectivity is in a similar range.

Experiments with compound **3c** as the catalyst and with cocatalysts other than MMAO showed a dramatic change of the activity. Thus, a cocatalyst mixture of $AlEt_3/B(C_6F_5)_3$ (7200:96) (Table 1, run 2) and $AlMe_3/B(C_6F_5)_3$ (7200:96) (Table 1, run 3) resulted in low yields of the desired product. Similar low performances were observed for the cocatalyst mixtures of $AlEt_3/[Ph_3C][B(C_6F_5)_4]$ (7200:96) (Table 1, run 4) and $[PhNMe_2H][B(C_6F_5)_4]$ (7200:85.9) (Table 1, run 5). In contrast, the use of the recently invented cocatalyst $[R_2NH][B(C_6F_5)_4]$ (Table 1, runs 6 and 7) resulted in a tremendous increase in activity. In particular, the cocatalyst mixture of $AlMe_3/[R_2(Ph)NH][B(C_6F_5)_4]$ (R = *N, N*-dioctadecylanilinium tetrakis(pentafluorophenyl)borate)[36]

Table 1. 1,3-Butadiene polymerization with complex **3c**.[a,b]

	Run number						
	1	2	3	4	5	6	7
catalyst [μmol]	24.09	24.00	24.00	24.00	24.00	24.00	24.00
MMAO [mmol]	14						
$AlEt_3$ [mmol]		7.2		7.2	7.2	7.2	
$B(C_6F_5)_3$ [μmol]		96	96				
$AlMe_3$ [mmol]			7.2				7.2
$[Ph_3C][B(C_6F_5)_4]$ [μmol]				96			
$[PhNMe_2H][B(C_6F_5)_4]$ [μmol]					85.9		
$[R_2(Ph)NH][B(C_6F_5)_4]$ [μmol]						93.2	93.2
1,3-butadiene [mol]	1.000	1.059	0.975	1.063		0.998	0.994
1,3-butadiene/Nd molar ratio	20832	22063	20310	22142	19754	20794	20717
butadiene conversion (10 min) [%]	14.5	10.7	3.2	2.4	2.1	21.9	88.7
butadiene conversion (1 h) [%]	86.1	15	5.4	4.2	6.3	51.6	99.8
activity[c]	0.981	0.766	0.211	0.172	0.135	1.478	5.965
cis-1,4-PBR[d] [%]	94.8					94.3	93.1
trans-1,4-PBR[d] [%]	0.7					4.1	5.5
1,2-PBR[d] [%]	4.5					1.6	1.4
M_w [g mol^{-1}]	610000					688000	696000
M_n [g mol^{-1}]	287000					237000	359000
D[e]	2.1					2.9	1.9
T_g [°C]						−108.1	−107.5

[a] The polymerization experiments were performed at Dow Olefinverbund GmbH. [b] Reaction temperature = 65 °C, solvent = cyclohexane. [c] Activity per kg of polymer per mmol of **3c** or **2** per hour, based on the result after 10 min. [d] PBR = polybutadiene. [e] D = polydispersity.

(7.2:93.2) gave more than a six-fold increase in activity (5.965 kg polymer per mmol catalyst·h) relative to MMAO, but with a similar *cis* selectivity (93.1%).

Conclusion

We have synthesized the first cyclodiphosph(III)azane complexes of the rare-earth elements. By using *cis*-[(*t*BuNP)$_2$(*t*BuN)$_2${Li(thf)}$_2$] as a transfer reagent two different types of metallate complexes were obtained, depending on the ionic radii of the metal centers. Complexes of the composition [Li(thf)$_4$][{(*t*BuNP)$_2$(*t*BuN)$_2$}LnCl$_2$] were obtained for the smaller rare-earth metals, whereas a trimetallic complex of the composition [{(*t*BuNP)$_2$(*t*BuN)$_2$}SmCl$_3$Li$_2$(thf)$_4$] was obtained for the larger samarium ion. Heating of the metalate complexes in toluene led to the extrusion of lithium chloride and the formation of the neutral metal chloride complexes of the composition [(*t*BuNP)$_2$(*t*BuN)$_2$LnCl(thf)]$_2$. In contrast to the metalate complexes, the neutral metal chlorides are all isostructural in the solid state. Furthermore, the reaction of [Li(thf)$_4$][{(*t*BuNP)$_2$(*t*BuN)$_2$}YCl$_2$] with KNPh$_2$ resulted in a lithium metalate complex of composition [Li(thf)$_4$][{(*t*BuNP)$_2$(*t*BuN)$_2$}Y(NPh$_2$)$_2$] instead of the desired neutral complex. The coordination of the {(*t*BuNP)$_2$(*t*BuN)$_2$}$^{2-}$ ligand in the latter compound is different from all other structures described in this contribution. Instead of the symmetric coordination of the yttrium atom above the center of the N$_2$P$_2$ plane, a heterocubane-type structure is observed in the solid state. The complex [(*t*BuNP)$_2$(*t*BuN)$_2$NdCl(thf)] was used as a Ziegler–Natta catalyst for the polymerization of 1,3-butadiene to poly-*cis*-1,4-butadiene. The observed activities are strongly dependent on the nature of the cocatalyst; in some case very high turnover rates and a *cis* selectivity of 93–94% were observed.

Since the cyclodiphosph(III)azane ligand can be considered as an alternative to the bridged biscyclopentadienyl ligands in *ansa*-metallocenes, we will continue to further establish their f element chemistry, which may give rise to new kinds of post-metallocene catalysts in the future.

Experimental Section

General: All manipulations of air-sensitive materials were performed with the rigorous exclusion of oxygen and moisture in flame-dried Schlenk-type glassware either on a dual manifold Schlenk line interfaced to a high vacuum (10^{-4} torr), or in an argon-filled M. Braun glove box. Solvents were predried over sodium wire and distilled under nitrogen from potassium (THF) or sodium wire (diethyl ether) and benzophenone ketyl prior to use; hydrocarbon solvents (toluene and *n*-pentane) were distilled under nitrogen from LiAlH$_4$. All solvents for vacuum line manipulations were stored in vacuo over LiAlH$_4$ in resealable flasks. Deuterated solvents were obtained from Chemotrade Chemiehandelsgesellschaft GmbH (all $\geq$99 atom% D) and were degassed, dried, and stored in vacuo over Na/K alloy in resealable flasks. NMR spectra were recorded on a JNM-LA 400 FT-NMR spectrometer. Chemical shifts are reported relative to tetramethylsilane (^{1}H NMR) and 85% phosphoric acid (^{31}P NMR). IR spectra were obtained on a Shimadzu FTIR-8400s. Elemental analyses were carried out with an Elementar vario EL instrument. LnCl$_3$,[37] {(*t*BuNP)$_2$(*t*BuNH)$_2$},[18] and *cis*-[(*t*BuNP)$_2$(*t*BuN)$_2${Li(thf)}$_2$][18] were prepared according to literature procedures.

General procedure for the synthesis of [Li(thf)$_4$][{(*t*BuNP)$_2$(*t*BuN)$_2$}LnCl$_2$] (Ln = Y (1a), Ho (1b), Er (1c)): THF (20 mL) was condensed at −196°C onto a mixture of LnCl$_3$ (0.80 mmol) and *cis*-[(*t*BuNP)$_2$(*t*BuN)$_2${Li(thf)}$_2$] (0.40 g, 0.80 mmol) and the mixture was stirred for 12 h at room temperature. The solvent was then evaporated in vacuo and toluene (20 mL) condensed onto the mixture. The mixture was filtered and the solvent was removed in vacuo. The product was recrystallized from THF/*n*-pentane (1:3).

1a: Yield: 0.21 g (27%); colorless crystals; ^{1}H NMR ([D$_8$]THF, 400 MHz, 20°C): δ = 2.71 (s, 18H; *t*Bu), 2.91 (s, 18H; *t*Bu); ^{31}P{^{1}H} NMR ([D$_8$]THF, 161.7 MHz, 20°C): δ = 91.6 ppm (s); FT Raman: 134 (m), 155 (s), 247 (s), 351 (w), 474 (m), 536 (m), 762 (w), 801 (w), 912 (w), 1223 (m), 1449 (m), 2897 (s), 2921 (s), 2962 cm^{-1} (s, νCH); elemental analysis calcd (%) for C$_{20}$H$_{44}$Cl$_2$LiN$_4$OP$_2$Y (584.16) (**1a**−3THF): C 41.04, H 7.58, N 9.57; found: C 40.98, H 7.65, N 9.49.

1b: Yield: 0.13 g (18%); yellow crystals; FT Raman: 119 (m), 133 (m), 156 (s), 240 (s), 350 (w), 473 (m), 536 (m), 764 (w), 802 (w), 912 (w), 1223 (m), 1449 (m), 2897 (s), 2921 (s), 2962 cm^{-1} (s, νCH); elemental analysis calcd (%) for C$_{20}$H$_{44}$Cl$_2$HoLiN$_4$OP$_2$ (661.31) (**1b**−3THF): C 36.32, H 6.71, N 8.47; found: C 35.72, H 6.61, N 8.17.

1c: Yield: 0.04 g (5%); pink crystals; FT Raman: 118 (m), 133 (m), 156 (s), 240 (s), 350 (w), 473 (m), 536 (m), 764 (w), 802 (w), 912 (w), 1223 (m), 1449 (m), 2896 (s), 2921 (s), 2962 cm^{-1} (s, νCH); elemental analysis calcd (%) for C$_{20}$H$_{44}$Cl$_2$ErLiN$_4$OP$_2$ (663.6) (**1c**−3THF): C 36.20, H 6.68, N 8.44; found: C 35.68, H 6.69, N 8.34.

[{(*t*BuNP)$_2$(*t*BuN)$_2$}SmCl$_3$Li$_2$(thf)$_4$] (2): THF (20 mL) was condensed at −196°C onto a mixture of SmCl$_3$ (0.21 g, 0.80 mmol) and *cis*-[(*t*BuNP)$_2$(*t*BuN)$_2${Li(thf)}$_2$] (0.40 g, 0.80 mmol) and the mixture was stirred for 12 h at room temperature. The solvent was then evaporated in vacuo and toluene (20 mL) condensed onto the mixture. The mixture was filtered and the solvent was removed in vacuo. The product was recrystallized from THF/*n*-pentane (1:3) to give **2** as light yellow crystals (0.22 g, 30%). FT Raman: 121 (m), 151 (s), 238 (s), 347 (w), 471 (s), 535 (s), 761 (s), 801 (s), 911 (m), 1222 (w), 1449 (m), 2896 (m), 2922 (s), 2962 cm^{-1} (s, νCH); elemental analysis calcd (%) for C$_{20}$H$_{44}$Cl$_3$Li$_2$N$_4$OP$_2$Sm (689.14) (**2**−3THF): C 34.86, H 6.44, N 8.13; found: C 33.80, H 6.75, N 7.64.

General procedure for the synthesis of [{(*t*BuNP)$_2$(*t*BuN)$_2$}LnCl(thf)]$_2$ (Ln=Y (3a), La (3b), Nd (3c), Sm (3d)): THF (20 mL) was condensed at −196°C onto a mixture of LnCl$_3$ (0.80 mmol) and *cis*-[(*t*BuNP)$_2$(*t*BuN)$_2${Li(thf)}$_2$] (0.40 g, 0.80 mmol) and the mixture was stirred for 12 h at room temperature. (Compound **3c** was reacted at 70°C). The solvent was then evaporated in vacuo and toluene (20 mL) condensed onto the mixture. The mixture was heated under reflux for a short period of time and the hot solution was filtered. The product was recrystallized from the mother solution.

3a: Yield: 0.07 g (15%); colorless crystals; ^{1}H NMR ([D$_8$]THF, 400 MHz, 20°C): δ = 1.23 (s, 36H; *t*Bu), 1.37 (s, 36H; *t*Bu); ^{31}P{^{1}H} NMR ([D$_8$]THF, 161.7 MHz, 20°C): δ = 99.7 ppm (s); FT Raman (single crystal): 119 (s), 260 (m), 533 (w), 548 (w), 607 (w), 743 (m), 810 (w), 914 (m), 1033 (w), 1225 (m), 1448 (s), 1464 (s), 2912 (s), 2926 (s), 2971 cm^{-1} (s, νCH); elemental analysis calcd (%) for C$_{32}$H$_{72}$Cl$_2$N$_8$P$_4$Y$_2$ (941.58) (**3a**−2THF): C 40.82, H 7.71, N 11.90; found: C 40.97, H 7.62, N 9.50.

3b: Yield: 0.09 g (18%); colorless crystals; ^{1}H NMR ([D$_8$]THF, 400 MHz, 20°C): δ = 1.24 (s, 36H; *t*Bu), 1.35 ppm (s, 36H; *t*Bu); ^{31}P{^{1}H} NMR ([D$_8$]THF, 161.7 MHz, 20°C): δ = 93.2 ppm; FT Raman (single crystal): 118 (s), 264 (m), 533 (w), 546 (w), 603 (w), 743 (m), 811 (w), 913 (m), 1030 (w), 1222 (m), 1447 (s), 1461 (s), 2912 (s), 2928 (s), 2971 cm^{-1} (s, νCH); elemental analysis calcd (%) for C$_{40}$H$_{88}$Cl$_2$La$_2$N$_8$O$_2$P$_4$ (1185.78): C 40.52, H 7.48, N 9.45; found: C 40.52, H 7.17, N 9.80.

3c: Yield: 0.09 g (18%); blue crystals; FT Raman (single crystal): 534 (w), 760 (m), 801 (w), 1222 (m), 1239 (m), 1449 (s), 2894 (s), 2919, 2961 cm^{-1} (s, νCH); elemental analysis calcd (%) for C$_{40}$H$_{88}$Cl$_2$N$_8$Nd$_2$O$_2$P$_4$ (1052.26): C 40.15, H 7.41, N 9.37; found: C 40.04, H 7.57, N 9.59.

3d: Yield: 0.10 g (20%); yellow crystals; FT Raman (single crystal): 118 (s), 260 (m), 533 (w), 543 (w), 603 (w), 742 (m), 808 (w), 915 (m), 1032 (w), 1222 (m), 1448 (s), 1461 (s), 2910 (s), 2925 (s), 2972 cm^{-1} (s, νCH); elemental analysis calcd (%) for $C_{40}H_{88}Cl_2N_8O_2P_4Sm_2$ (1208.7): C 39.75, H 7.34, N 9.27; found: C 41.20, H 8.08, N 10.41.

$[Li(thf)_4][\{(tBuNP)_2(tBuN)_2\}Y(NPh_2)_2]$ (4): THF (20 mL) was condensed at −196°C onto a mixture of $[Li(thf)_4][\{(tBuNP)_2(tBuN)_2\}YCl_2]$ (**1a**; 0.86 g, 0.80 mmol) and $KNPh_2$ (0.33 g, 1.60 mmol) and the mixture was stirred for 12 h at room temperature. The solvent was then evaporated in vacuo and toluene (20 mL) condensed onto the mixture. The mixture was filtered and the solvent was removed in vacuo. The product was recrystallized from THF/*n*-pentane (1:3) to give **4** as yellow crystals (0.20 g, 24%). ^1H NMR (C_6D_6, 400 MHz, 20°C): $\delta = 1.00$ (s, 18H; *t*Bu), 1.22 (s, 18H; *t*Bu), 1.55–1.65 (m, 16H; THF), 3.45–3.55 (m, 16H; THF), 6.23–6.91 ppm (m, 20H; Ph); $^{31}P\{^1H\}$ NMR (C_6D_6, 161.7 MHz, 20°C): $\delta =$ 127.6 ppm (s); FT Raman: 103 (s), 118 (s), 214 (m), 318 (w), 411 (w), 523 (m), 535 (w), 646 (m), 865 (w), 985 (s), 995 (m), 1027 (m), 1149 (w), 1205 (w), 1448 (w), 1575 (m), 1591 (m), 2891 (m), 2919 (m), 2958 (m), 3021 (w), 2048 cm^{-1} (m); elemental analysis calcd (%) for $C_{56}H_{88}LiN_6O_4P_2Y$ (1067.13): C 63.02, H 8.31, N 7.88; found: C 62.55, H 9.81, N 7.76.

1,3-Butadiene polymerization: The polymerization experiments were carried out in a double-walled steel reactor at +65°C in cyclohexane. The polymerization was initiated by addition of the lanthanide complex to a solution of 1,3-butadiene in cyclohexane and the activator MMAO (290 equiv). For the termination of the polymerization process, the polymer solution was transferred into a solution in methanol that contained Irganox 1520 as a polymer stabilizer. The microstructure of the polybutadiene was analyzed spectroscopically.

The products were characterized by means of size exclusion chromatography (SEC) by using an Autosampler 717 plus (Waters) instrument. Injection volume = 150 μL; G1310A IsoPump of Agilent 1100 series; flow rate = 0.80 mL min^{-1}; Triple Detector Array TriSEC Model 302 (Viscotek); DG-2410 Degasser (Uniflows); OmniSEC software, version 3.1; 3 and 2 PLgel 20 μm MIXED-A (1110–6200) + 1 PLgel 20 μm MIXED-ALS (1110–6200 LS), Polymer Laboratories. M_n and M_w were determined by a universal calibration of SEC against a polystyrene standard (PS standard 111 000 g mol^{-1} (Waters, No. 41995)). The ratio between the 1,4-*cis*, 1,4-*trans*, and 1,2-polydiene contents of the butadiene was determined by ^{13}C NMR spectroscopy.

X-ray crystallographic studies of 1a–c, 2, 3a–d, and 4: Crystals of **1a–c**, **2** and **4** were grown from THF/*n*-pentane (1:2). Crystals of **3a–d** were obtained from the mother solution. A suitable crystal was covered in mineral oil (Aldrich) and mounted onto a glass fiber. The crystal was transferred directly to the −73°C N_2 cold stream of a Stoe IPDS II diffractometer. Subsequent computations were carried out on an Intel Pentium IV PC.

All structures were solved by the Patterson method (SHELXS-97[38]). The remaining non-hydrogen atoms were located from successive difference Fourier map calculations. The refinements were carried out with the use of full-matrix least-squares techniques on *F*, minimizing the function $(F_o-F_c)^2$, in which the weight is defined as $4F_0^2/2(F_o^2)$, and F_o and F_c are the observed and calculated structure factor amplitudes obtained by using the program SHELXL-97.[39] Carbon-bound hydrogen atom positions were calculated and allowed to ride on the carbon to which they are bonded by assuming a C–H bond length of 0.95 Å. The hydrogen atom contributions were calculated, but not refined. The locations of the largest peaks in the final difference Fourier map calculation as well as the magnitude of the residual electron densities in each case were of no chemical significance. CCDC-670362, 670363, 670364, 670365, 670366, 670367, 670368, 670369, and 670370 contain the supplementary crystallographic data for this paper. These data can be obtained free of charge from The Cambridge Crystallographic Data Centre via www.ccdc.cam.ac.uk/data_request/cif.

1a: $C_{32}H_{68}Cl_2LiN_4O_4P_2Y$; orthorhombic; *Pbca* (No. 61); lattice constants $a = 1837.54(14)$, $b = 2538.48(14)$, $c = 1896.68(14)$ pm; $V = 8847.2(11) \times 10^6$ pm^3; $Z = 8$; $\mu(Mo_{K\alpha}) = 1.546$ mm^{-1}; $\theta_{max.} = 25°$; 7702 [$R_{int} = 0.0863$] independent reflections measured, of which 4886 were considered observed with $I > 2\sigma(I)$; max. residual electron density 0.541 and −0.523 e A^{-3}; 414 parameters, *R*1 ($I > 2\sigma(I)$) = 0.0766; w*R*2 (all data) = 0.1673.

1b $C_{32}H_{68}Cl_2ErLiN_4O_4P_2$; orthorhombic; *Pbca* (No. 61); lattice constants $a = 1835.43(13)$, $b = 2529.95(11)$, $c = 1892.82(11)$ pm; $V = 8789.4(9) \times 10^6$ pm^3; $Z = 8$; $\mu(Mo_{K\alpha}) = 2.139$ mm^{-1}; $\theta_{max.} = 27.5°$; 10075 [$R_{int} = 0.0436$] independent reflections measured, of which 5908 were considered observed with $I > 2\sigma(I)$; max. residual electron density 0.541 and −0.847 e A^{-3}; 412 parameters, *R*1 ($I > 2\sigma(I)$) = 0.0293; w*R*2 (all data) = 0.0670.

1c: $C_{32}H_{68}Cl_2HoLiN_4O_4P_2$; orthorhombic; *Pbca* (No. 61); lattice constants $a = 1836.23(9)$, $b = 2531.33(11)$, $c = 1893.45(9)$ pm; $V = 8801.0(7) \times 10^6$ pm^3, $Z = 8$; $\mu(Mo_{K\alpha}) = 2.027$ mm^{-1}; $\theta_{max.} = 25$; 7661 [$R_{int} = 0.0323$] independent reflections measured, of which 5545 were considered observed with $I > 2\sigma(I)$; max. residual electron density 0.579 and −0.981 e A^{-3}; 418 parameters, *R*1 ($I > 2\sigma(I)$) = 0.0278; w*R*2 (all data) = 0.0671.

2: $C_{32}H_{68}Cl_3Li_2N_4O_4P_2Sm$; monoclinic, $P2_1/c$ (No. 14); lattice constants $a = 1098.80(7)$, $b = 2350.01(13)$, $c = 1801.15(10)$ pm; $\beta = 98.250(5)°$; $V = 4602.8(5) \times 10^6$ pm^3, $Z = 4$; $\mu(Mo_{K\alpha}) = 1.554$ mm^{-1}; $\theta_{max.} = 25$; 8066 [R_{int}0.0591] independent reflections measured, of which 5082 were considered observed with $I > 2\sigma(I)$; max. residual electron density 0.823 and −0.623 e A^{-3}; 335 parameters, *R*1 ($I > 2\sigma(I)$) = 0.0501; w*R*2 (all data) = 0.1256.

3a: $C_{40}H_{88}Cl_2N_8O_2P_4Y_2$; triclinic; $P\bar{1}$ (No. 2); lattice constants $a = 1033.98(7)$, $b = 1045.58(8)$, $c = 1344.50(9)$ pm; $\alpha = 107.784(5)$, $\beta = 100.043(5)$, $\gamma = 90.058(6)°$; $V = 1360.6(2) \times 10^6$ pm^3, $Z = 1$; $\mu(Mo_{K\alpha}) = 2.367$ mm^{-1}; $\theta_{max.} = 25$; 4796 [$R_{int} = 0.0395$] independent reflections measured, of which 4251 were considered observed with $I > 2\sigma(I)$; max. residual electron density 0.663 and −0.607 e A^{-3}; 256 parameters, *R*1 ($I > 2\sigma(I)$) = 0.0397; w*R*2 (all data) = 0.0946.

3b: $C_{40}H_{88}Cl_2La_2N_8O_2P_4$; triclinic; $P\bar{1}$ (No. 2); lattice constants $a = 1034.1(7)$, $b = 1050.0(5)$, $c = 1362.5(7)$ pm; $\alpha = 74.00(4)$, $\beta = 81.51(5)$, $\gamma = 89.40(5)°$; $V = 1405.9(13) \times 10^6$ pm^3, $Z = 1$; $\mu(Mo_{K\alpha}) = 1.745$ mm^{-1}; $\theta_{max.} = 25$; 4891 [$R_{int} = 0.0904$] independent reflections measured, of which 4134 were considered observed with $I > 2\sigma(I)$; max. residual electron density 1.325 and −1.513 e A^{-3}; 275 parameters, *R*1 ($I > 2\sigma(I)$) = 0.0534; w*R*2 (all data) = 0.1325.

3c: $C_{40}H_{88}Cl_2N_8Nd_2O_2P_4$; triclinic, $P\bar{1}$ (No. 2); lattice constants $a = 1032.23(7)$, $b = 1048.14(7)$, $c = 1353.57(9)$ pm; $\alpha = 73.123(5)$, $\beta = 81.51(5)$, $\gamma = 80.780(5)°$; $V = 1381.78(16) \times 10^6$ pm^3; $Z = 1$; $\mu(Mo_{K\alpha}) = 2.108$ mm^{-1}; $\theta_{max.} = 25$; 4869 [$R_{int} = 0.0266$] independent reflections measured, of which 4615 were considered observed with $I > 2\sigma(I)$; max. residual electron density 2.858 and −1.602 e A^{-3}; 275 parameters, *R*1 ($I > 2\sigma(I)$) = 0.0349; w*R*2 (all data) = 0.0925.

3d: $C_{40}H_{88}Cl_2N_8O_2P_4Sm_2$; triclinic, $P\bar{1}$ (No. 2); lattice constants $a = 1033.15(7)$, $b = 1048.98(7)$, $c = 1350.15(9)$ pm; $\alpha = 72.824(5)$, $\beta = 80.453(5)$, $\gamma = 89.833(6)°$; $V = 1377.0(2) \times 10^6$ pm^3, $Z = 2$; $\mu(Mo_{K\alpha}) = 2.363$ mm^{-1}; $\theta_{max.} = 25$; 4846 [$R_{int} = 0.0249$] independent reflections measured, of which 4494 were considered observed with $I > 2\sigma(I)$; max. residual electron density 1.483 and 0.688 e A^{-3}; 275 parameters, *R*1 ($I > 2\sigma(I)$) = 0.0252; w*R*2 (all data) = 0.0617.

4: $C_{56}H_{88}LiN_6O_4P_2Y$; monoclinic; $P2_1/c$ (No. 14); lattice constants $a = 1424.59(9)$, $b = 1779.70(14)$, $c = 2330.24(15)$ pm; $\beta = 93.323(5)°$; $V = 5898.0(7) \times 10^6$ pm^3, $Z = 4$; $\mu(Mo_{K\alpha}) = 1.090$ mm^{-1}; $\theta_{max.} = 25$; 10174 [$R_{int} = 0.0705$] independent reflections measured, of which 4584 were considered observed with $I > 2\sigma(I)$; max. residual electron density 0.677 and −0.456 e A^{-3}; 481 parameters, *R*1 ($I > 2\sigma(I)$) = 0.0677; w*R*2 (all data) = 0.1774.

Acknowledgements

This work was supported by the Deutsche Forschungsgemeinschaft. R.B.M. gratefully acknowledges a fellowship of the Deutscher Akademischer Austauschdienst (DAAD) and CAPES. Dow Olefinverbund GmbH is acknowledged for performing the polymerization experiments.

[1] For reviews, see: a) F. T. Edelmann, *Angew. Chem.* **1995**, *107*, 2647–2669; *Angew. Chem. Int. Ed. Engl.* **1995**, *34*, 2466–2488; b) F. T. Edelmann, D. M. M. Freckmann, H. Schumann, *Chem. Rev.* **2002**, *102*, 1851–1896; c) M. Konkol, J. Okuda, *Coord. Chem. Rev.* **2008**, *252*, 1577–1591.

[2] For reviews, see: a) G. J. P. Britovsek, V. C. Gibson, D. F. Wass, *Angew. Chem.* **1999**, *111*, 448–468; *Angew. Chem. Int. Ed.* **1999**, *38*, 428–447; b) R. Kempe, *Angew. Chem.* **2000**, *112*, 478–504; *Angew. Chem. Int. Ed.* **2000**, *39*, 468–493; c) W. E. Piers, D. J. H. Emslie, *Coord. Chem. Rev.* **2002**, *233–234*, 131–155; d) F. T. Edelmann, *Adv. Organomet. Chem.* **2008**, *57*, 183–352.

[3] a) T. G. Wetzel, S. Dehnen, P. W. Roesky, *Angew. Chem.* **1999**, *111*, 1155–1158; *Angew. Chem. Int. Ed.* **1999**, *38*, 1086–1088; b) S. Wingerter, M. Pfeiffer, F. Baier, T. Stey, D. Stalke, *Z. Anorg. Allg. Chem.* **2000**, *626*, 1121–1130.

[4] a) S. Anfang, K. Harms, F. Weller, O. Borgmeier, H. Lueken, H. Schilder, K. Dehnicke, *Z. Anorg. Allg. Chem.* **1998**, *624*, 159–166; b) S. Anfang, T. Gröb, K. Harms, G. Seybert, W. Massa, A. Greiner, K. Dehnicke, *Z. Anorg. Allg. Chem.* **1999**, *625*, 1853–1859; c) T. Gröb, G. Seybert, W. Massa, F. Weller, R. Palaniswami, A. Greiner, K. Dehnicke, *Angew. Chem.* **2000**, *112*, 4542–4544; *Angew. Chem. Int. Ed.* **2000**, *39*, 4373–4375; d) T. Gröb, G. Seybert, W. Massa, K. Dehnicke, *Z. Anorg. Allg. Chem.* **2001**, *627*, 304–306.

[5] P. W. Roesky, M. T. Gamer, M. Puchner, A. Greiner, *Chem. Eur. J.* **2002**, *8*, 5265–5271.

[6] a) M. T. Gamer, G. Canseco-Melchor, P. W. Roesky, *Z. Anorg. Allg. Chem.* **2003**, *629*, 2113–2116; b) P. W. Roesky, M. T. Gamer, N. Marinos, *Chem. Eur. J.* **2004**, *10*, 3537–3542; c) M. T. Gamer, P. W. Roesky, *Inorg. Chem.* **2004**, *43*, 4903–4906; d) P. W. Roesky, *Inorg. Chem.* **2006**, *45*, 798–802.

[7] a) M. T. Gamer, S. Dehnen, P. W. Roesky, *Organometallics* **2001**, *20*, 4230–4236; b) M. T. Gamer, P. W. Roesky, *J. Organomet. Chem.* **2002**, *647*, 123–127.

[8] K. Aparna, M. Furguson, R. G. Cavell, *J. Am. Chem. Soc.* **2000**, *122*, 726–727.

[9] a) F. T. Edelmann, *Top. Curr. Chem.* **1996**, *179*, 113–148; b) U. Reissmann, P. Poremba, M. Noltemeyer, H.-G. Schmidt, F. T. Edelmann, *Inorg. Chim. Acta* **2000**, *303*, 156–162; c) A. Recknagel, A. Steiner, M. Noltemeyer, S. Brooker, D. Stalke, F. T. Edelmann, *J. Organomet. Chem.* **1991**, *414*, 327–335; d) A. Recknagel, M. Witt, F. T. Edelmann, *J. Organomet. Chem.* **1989**, *371*, C40-C44.

[10] a) S. Agarwal, C. Mast, K. Dehnicke, A. Greiner, *Macromol. Rapid Commun.* **2000**, *21*, 195–212; b) P. Ravi, T. Groeb, K. Dehnicke, A. Greiner, *Macromolecules* **2001**, *34*, 8649–8653.

[11] M. T. Gamer, P. W. Roesky, A. Steffens, M. Glanz, *Chem. Eur. J.* **2005**, *11*, 3165–3172.

[12] a) A. Zulys, T. K. Panda, M. T. Gamer, P. W. Roesky, *Chem. Commun.* **2004**, 2584–2585; b) A. Zulys, T. K. Panda, M. T. Gamer, P. W. Roesky, *Organometallics* **2005**, *24*, 2197–2202.

[13] M. Rastätter, A. Zulys, P. W. Roesky, *Chem. Commun.* **2006**, 874–876.

[14] a) A. Michaelis, G. Schroeter, *Ber. Dtsch. Chem. Ges.* **1894**, *27*, 490–497; b) A. Michaelis, *Annalen* **1903**, *326*, 129–258.

[15] K. W. Muir, J. F. Nixon, *J. Chem. Soc. D* **1971**, *21*, 1405–1406.

[16] E. Niecke, W. Flick, S. Pohl, *Angew. Chem.* **1976**, *88*, 305–306; *Angew. Chem. Int. Ed. Engl.* **1976**, *15*, 309–310.

[17] a) R. R. Holmes, *J. Am. Chem. Soc.* **1961**, *83*, 1334–1336; b) T. G. Hill, R. C. Haltiwanger, M. L. Thompson, S. A. Katz, A. D. Norman, *Inorg. Chem.* **1994**, *33*, 1770–1777.

[18] I. Schranz, L. Stahl, R. J. Staples, *Inorg. Chem.* **1998**, *37*, 1493–1498.

[19] L. Stahl, *Coord. Chem. Rev.* **2000**, *210*, 203–250.

[20] M. Rastätter, P. W. Roesky, D. Gudat, G. B. Deacon, P. C. Junk, *Chem. Eur. J.* **2007**, *13*, 7410–7415.

[21] a) L. P. Grocholl, L. Stahl, R. J. Staples, *Chem. Commun.* **1997**, 1465–1466; b) D. F. Moser, C. J. Carrow, L. Stahl, R. J. Staples, *J. Chem. Soc. Dalton Trans.* **2001**, 1246–1252; c) D. F. Moser, L. Grocholl, L. Stahl, R. J. Staples, *Dalton Trans.* **2003**, 1402–1410; d) K. V. Axenov, M. Klinga, M. Leskelä, V. V. Kotov, T. Repo, *Eur. J. Inorg. Chem.* **2004**, 695–706; e) K. V. Axenov, M. Klinga, M. Leskelä, V. V. Kotov, T. Repo, *Eur. J. Inorg. Chem.* **2004**, 4702–4709.

[22] K. V. Axenov, M. Klinga, M. Leskelä, T. Repo, *Organometallics* **2005**, *24*, 1336–1343.

[23] review: H. Schumann, J. A. Meese-Marktscheffel, L. Esser, *Chem. Rev.* **1995**, *95*, 865–986.

[24] W. J. Evans, J. Olofson, H. Zhang, J. L. Atwood, *Organometallics* **1988**, *7*, 62–633.

[25] T. G. Wetzel, S. Dehnen, P. W. Roesky, *Angew. Chem.* **1999**, *111*, 1155–1158; *Angew. Chem. Int. Ed.* **1999**, *38*, 1086–1088.

[26] E. Ihara, M. Tanaka, H. Yasuda, N. Kanehisa, T. Maruo, Y. Kai, *J. Organomet. Chem.* **2000**, *613*, 26–32.

[27] W. J. Evans, R. A. Keyer, J. W. Ziller, *Organometallics* **1993**, *12*, 2618–2633.

[28] A. D. Bond, E. L. Doyle, F. Garcia, R. A. Kowenicki, D. Moncrieff, M. McPartlin, L. Riera, A. D. Woods, D. S. Wright, *Chem. Eur. J.* **2004**, *10*, 2271–2276.

[29] Y. Yao, X. Lu, Q. Shen, K. Yu, *J. Chem. Crystallogr.* **2004**, *34*, 275–279.

[30] a) J. Witte, *Angew. Makromol. Chem.* **1981**, *94*, 119–124; b) D. J. Wilson, *Polym. Int.* **1996**, *39*, 235–242; c) R. Taube, G. Sylvester in *Applied Homogeneous Catalysis with Organometallic Compounds* (Eds.: B. Cornils, W. A. Herrmann), VCH, Weinheim, **1996**, pp. 280–318; d) S. K.-H. Thiele, D. R. Wilson, *J. Macromol. Sci. Polym. Rev.* **2003**, *43*, 581–628.

[31] A. Fischbach, R. Anwander, *Adv Polym Sci* **2006**, *204*, 155–281.

[32] a) R. Taube, H. Windisch, S. Maiwald, H. Hemling, H. Schumann, *J. Organomet. Chem.* **1996**, *513*, 49–61; b) S. Maiwald, R. Taube, H. Hemling, H. Schumann, *J. Organomet. Chem.* **1998**, *552*, 195–204.

[33] V. Lorenz, H. Görls, S. K.-H. Thiele, J. Scholz, *Organometallics* **2005**, *24*, 797–800.

[34] D. J. Wilson, *Polym. Int.* **1996**, *39*, 235–242.

[35] H. Sugiyama, S. Gambarotta, G. P. A. Yap, D. R. Wilson, S. K.-H. Thiele, *Organometallics* **2004**, *23*, 5054–5061.

[36] J. C. Stevens, D. D. Vanderlende PCT Int. Appl. **2003**, WO 2003040201, CAN 138:385930.

[37] M. D. Taylor, C. P. Carter, *J. Inorg. Nucl. Chem.* **1962**, *24*, 387–391.

[38] G. M. Sheldrick, SHELXS-97, *Program of Crystal Structure Solution*, University of Göttingen, Göttingen (Germany), **1997**.

[39] G. M. Sheldrick, SHELXL-97, *Program of Crystal Structure Refinement*, University of Göttingen, Göttingen (Germany), **1997**.

Received: March 3, 2008
Revised: September 24, 2008
Published online: November 25, 2008

